Available online at www.sciencedirect.com

ScienceDirect

IFAC Papers Online CONFERENCE PAPER ARCHIVE

IFAC PapersOnLine 55-25 (2022) 25–30

Observer-based gust load alleviation via reduced-order models ⋆

Alex dos Reis de Souza *, **Pierre Vuillemin** *, **David Quero** **, **Charles Poussot-Vassal** *

* *Onera – The French Aerospace Lab. 2 Avenue Edouard Belin, Toulouse 31400, France.*

** *DLR (German Aerospace Center), Institute of Aeroelasticity, Bunsenstraße 10, 37073 Göttingen, Germany.*

Abstract: In this paper, we investigate the design of linear active output feedback control for aircraft gust load alleviation, involving standard sensors and control surfaces. The control architecture is composed of *(i)* a robust observer, allowing for estimating some wing bending moments despite the wind perturbation, and *(ii)* a structured $\mathcal{H}_\infty$-norm oriented control law exploiting this additional information. To cope with the complexity of the aeroelastic model and make the control and observer synthesis computationally tractable, a model reduction step, based on Petrov-Galerkin projections, is first applied. One specificity of this work is that the obtained projector is exploited in the observer design, linking the reduction and the estimation. The effectiveness of the methodology is illustrated through numerical simulation involving an open access high complexity aeroelastic model.

Keywords: Estimation, Robust control, Projection-based, Model reduction, Aircraft control

1. INTRODUCTION

The alleviation of structural efforts along the wing of an aircraft is an important feature in aeronautics. Indeed, this feature is responsible for extending the life span of the structure, as well as reducing the aircraft fuel consumption during its exploitation. Moreover, it is a central element for aircraft certification by regulatory agencies.

Active control schemes for the alleviation of dynamic aircraft loads, such as the ones caused by atmospheric disturbances, have been an active field of research over the last decades (Regan and Jutte, 2012; Livne, 2018). Besides the certification requirements, the need for such schemes has also been motivated by the modern trend of designing more flexible or high-aspect-ratio aircraft (Regan and Jutte, 2012) with the objective of reducing fuel consumption.

However, this control problem is challenging for several practical and technical reasons. Since aircraft models that accurately describe the interaction between structural and aerodynamics are complex and high-dimensional (Karpel, 1982), the synthesis of controllers and state observers can become numerically troublesome. Therefore, model approximation and reduction are vital steps to address this complexity, since a proper control design will depend on a compromise between the accuracy and the dimension of the model used (Wang et al., 2016).

Despite these challenges, several control algorithms have been proposed for Gust Load Alleviation (GLA), *e.g.*, using Model Predictive Control (Giesseler et al., 2012), adaptive feed-forward (Zeng et al., 2010), robust control (Cook et al., 2013), control allocation (Hansen et al., 2020), among others. These works often rely on light detection and ranging (LIDAR) to sense turbulence. However, the latter technology is still under development, remaining expensive, heavy and not accurate enough to be included in a certified control loop.

The use of reduced-order models for observer design has also been addressed in the literature. For instance, Sadamoto et al. (2014) introduce projective observers as a generalization of functional observers, whereas in (Sadamoto et al., 2013), the same problem is dealt with by later approximating the observer. Steiner and Liu (2020) uses the Proper Orthogonal Decomposition to design a reduced-order observer for interconnected systems.

In this paper, we present a methodological approach for the design of an observer-based robust control scheme exploiting some load estimates in the gust load alleviation control law. This approach is validated on the high dimensional aeroelastic model proposed by Quero et al. (2019) [1], which can describe the bending moments over several points across the wing. In addition, given the large-scale settings, model-based reduction techniques are used *(i)* to account for the numerical complexity and simplify the observer and controller computation, and *(ii)* the resulting Petrov-Galerkin projectors (see Antoulas (2005)), embedded in the observer design step to account for neglected dynamics.

⋆ This work has been funded within the frame of the Joint Technology Initiative JTI Clean Sky 2, AIRFRAME Integrated Technology Demonstrator platform AIRFRAME ITD (contract N. CSJU-CS2-GAM-AIR-2014-15-01 Annex 1, Issue B04, October 2nd, 2015) being part of the Horizon 2020 research and Innovation framework program of the European Commission.

[1] The model is accessible at `http://pierre-vuillemin.fr/resources/ModelGLA.mat`.

10.1016/j.ifacol.2022.09.318

The overall scheme is composed of *(i)* a proportional-integral observer (PIO) Beale and Shafai (1989), which allows the robust estimation of the bending moments acting over the wing, and *(ii)* a structured $\mathcal{H}_\infty$ controller (Apkarian and Noll, 2006), which uses these estimates to alleviate the effect of these perturbations by attenuating its worst-case load transfer. Both syntheses are constrained to the reduced-order model. In addition, the observer design exploits the projector obtained in the model reduction step, which stands as an interesting feature of the proposed methodology.

Paper structure: Section 2 introduces the aircraft model, the considered assumptions, and the problem to be solved. Section 3 presents the design of the PIO and $\mathcal{H}_\infty$-norm oriented controller based on the reduced-order model and projector. Section 4 illustrates the methodology with a numerical open-access aeroelastic model and, finally, Section 5 concludes this study.

Notation: The set of real numbers of dimension n is denoted $\mathbb{R}^n$. The notations $\text{vec}(\cdot,\dots,\cdot)$ and $\text{diag}(\cdot,\dots,\cdot)$ represent, respectively, the composition of its arguments into a vector and into a diagonal matrix (possibly composed by another matrices). The identity matrix of dimension n is represented by I_n. The infinity norm is represented by $|\cdot|_\infty$. The notation $\langle A\rangle$ stands for the symmetric matrix $A+A^\top$. The symmetric entry of a matrix, *i.e.*, $A_{ij}=A_{ji}^\top$ is denoted by $\star$. The lower linear fractional transformation of a (generalized) plant P with a controller K is represented by $F_l(P,K)$. The function $\text{randn}(\mu,\sigma)$ returns a random value picked from a normal distribution with mean μ and standard deviation σ.

2. PRELIMINARIES

The model used in this study is described as follows:

$$\begin{aligned}\dot{x} &= Ax + Bu + Ew\\ y_m &= C_m x + D_{mv} v\\ y_l &= C_l x\end{aligned} \tag{1}$$

where $x\in\mathbb{R}^n$ is the state vector, $u\in\mathbb{R}^p$ is the control input, $y_m\in\mathbb{R}^m$ and $y_l\in\mathbb{R}^l$ are, respectively, measured and unmeasured outputs. The considered perturbations $w\in\mathbb{R}$ and $v\in\mathbb{R}$ are, respectively, the wind gust and measurement noise. The matrices A, B, C_m, C_l, D_{mv} and E are known and have proper dimensions.

In this work, system (1) describes an aeroelastic aircraft model, with dimensions $n=216$, $m=3$, $p=3$, and $l=47$. Furthermore, the outputs y_l represent the efforts (bending moments) acting along the wing span. These outputs are called *virtual* in the sense that they are not physically measured. Whenever needed, we denote $y_l^{(i)}$ as the bending moment acting on the i-th wing station, ranging from wing root to wing tip (*i.e.*, $y_l^{(1)}$ and $y_l^{(47)}$, respectively).

The available control inputs are conventional control surfaces, *i.e.*, $u=\text{vec}(\delta_{in},\delta_{ext},\delta_{elev})$, where δ_{in} and δ_{ext} are, respectively, the deflection of the wing's inner and outer ailerons, and δ_{elev} is deflection of the elevator. The measured outputs y_m are classic quantities obtained from inertial sensors located at the center of gravity of the aircraft, *i.e.*, $y_m=\text{vec}(\theta,\dot{z},\dot{\theta})$, where θ and z are, respectively, the pitch angle and the vertical displacement of the aircraft.

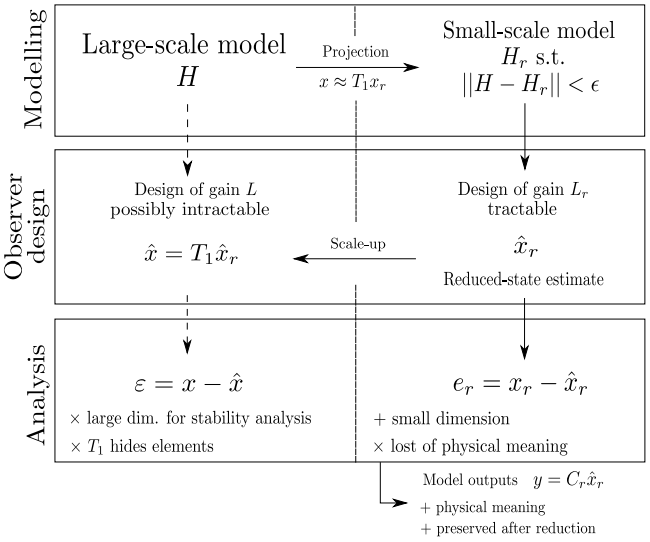

Fig. 1. Schematic representation of the overall observer synthesis process.

Problem 1: design an active control law that minimizes the (worst-case) transfer gain $w\mapsto y_l^{(1)}$.

Note that only the transfer regarding the bending moment acting on the wing root (*i.e.*, $y_l^{(1)}$) needs to be taken into account for control design. Indeed, as it will be illustrated later by a numerical example, this wing station is *always* the most solicited by bending efforts.

Problem 1 will be tackled as follows: first, a PIO will be designed in order to estimate $\hat{y}_l$, a subset of the (unmeasured) performance outputs y_l. Then, using this information and model (1), a structured $\mathcal{H}_\infty$ controller will be designed to robustly attenuate the affect of w into a subset of y_l.

3. DEVELOPMENT OF THE CONTROL ARCHITECTURE

3.1 Reduced-order models

The dimension of (1) is prohibitive for both observer and controller design. Therefore, model order reduction techniques may be applied to overcome this limitation. In the case of (1), a realization is available and thus projection-based reduction techniques, such as Balanced Truncation (BT), can be applied. Without deepening into details (the interested reader is invited to refer to (Antoulas, 2005)), this class of methods consists in determining two orthogonal Petrov-Galerkin projectors, $T_1\in\mathbb{R}^{n\times r}$ and $T_2\in\mathbb{R}^{n\times r}$, leading to a reduced-order version of (1) as given by:

$$\begin{aligned}\dot{x}_r &= A_r x_r + B_r u + E_r w\\ y_{m,r} &= C_{m,r} x_r\end{aligned} \tag{2}$$

where $A_r=T_2^\top A T_1\in\mathbb{R}^{r\times r}$, $B_r=T_2^\top B\in\mathbb{R}^{r\times m}$, $C_{m,r}=C_m T_1\in\mathbb{R}^{m\times r}$, and $E_r=T_2^\top E\in\mathbb{R}^r$. Following this notation, the original states can be retrieved, up to some approximation error induced by the reduction, by $x\approx T_1 x_r$. Notice that $y_{m,r}$ is merely the output of the reduced

model, not physically measured and, thus, considering it as affected by measurement noise is pointless.

Two different reduced-order models are to be distinguished in the following. Let us consider a subset $\tilde{y}$ of y_l consisting of the virtual outputs that will be estimated and used for control purposes. The reduction steps are as follows:

(1) For controller synthesis, model (1) is reduced to an order n_1 considering both y_m and $\tilde{y}$ ($\tilde{y}$ will be recovered by the PIO);
(2) For observer synthesis, model (1) is reduced to an order n_2, but considering solely y_m as measurements.

It is worth noticing that the orders n_1 and n_2 are not necessarily the same. Indeed, the observer might require a higher order to provide reliable estimates. Also, since the accuracy of the reduced-order model when describing the original one is affected by the number of outputs taken into account, not all elements of y_l need to be considered.

The reasons why y_l is neglected on the second reduced-order model are *(i)* since y_l is not measured, it cannot be used for output injection and thus is useless for observer design, and *(ii)* the difference of magnitude between y_l and y_m might induce numerical difficulties when computing the observer gains. It is worth noticing, however, that a mapping relating x_r to the performance outputs y_l is obtained by the *virtual* measurement matrix $C_{l,r} = C_l T_1$.

3.2 Observer design

Since the wind perturbation w is unknown, we need an observer that is able to estimate x_r (and, consequently, x) robustly. Following Beale and Shafai (1989), a PIO can be designed as

$$\begin{aligned} \dot{\hat{x}}_r &= A_r\hat{x}_r + B_r u + E_r\hat{w} + L_1\left(y_m - C_{m,r}\hat{x}_r\right) \\ \dot{\hat{w}} &= L_2\left(y_m - C_{m,r}\hat{x}_r\right) \end{aligned} \tag{3}$$

where $\hat{x}_r \in \mathbb{R}^r$ and $\hat{w}$ are, respectively, the estimates of x_r, and w, while $L_1 \in \mathbb{R}^{r\times p}$ and $L_2 \in \mathbb{R}^{1\times p}$ are gains to be determined.

Let $e = \mathrm{vec}(x_r - \hat{x}_r, w - \hat{w})$ and consider the exogenous perturbation vector as $d = \mathrm{vec}(v, \dot{w})$. After simple algebraic manipulation, the estimation error dynamics can be computed as:

$$\begin{aligned} \dot{e} &= \begin{bmatrix} A_r - L_1C_{m,r} & E_r \\ -L_2C_{m,r} & 0 \end{bmatrix} e + \begin{bmatrix} -L_1D_{mv} & 0 \\ -L_2D_{mv} & 1 \end{bmatrix} d \\ &= \left(\tilde{A} - \tilde{L}\tilde{C}\right) e + \left(\tilde{L}\tilde{D} + \tilde{I}\right) d \end{aligned} \tag{4}$$

where $\tilde{C} = [C_{m,r}\ 0]$, $\tilde{D} = [-D_{mv}\ 0]$, $\tilde{I} = \mathrm{diag}(0,1)$, $\tilde{L} = [L_1^\top, L_2^\top]^\top$, and $\tilde{A} = \begin{bmatrix} A_r & E_r \\ 0 & 0 \end{bmatrix}$.

Remark 1. Note that PIO (3) acts as a disturbance observer, in the sense that it will try to reconstruct w and compensate it in the error dynamics (4). However, disregarding the gains L_1, L_2, this reconstruction cannot be perfect, since the observer is built using the reduced model.

If (4) is stable, then x_r can be estimated and the bending moments are easily recovered by

$$\hat{y}_l = C_l T_1 \hat{x}_r. \tag{5}$$

The following result offers a way to design gains L_1 and L_2, and also an optimization criterion of the performance of the estimation.

Lemma 1. Consider the reduced-order system (2) and observer (3). Let $Q \in \mathbb{R}^2$ be a given symmetric and positive definite matrix. If there exist matrices $U_1 \in \mathbb{R}^{n_2\times p}$, $U_2 \in \mathbb{R}^{1\times p}$, and $P \in \mathbb{R}^{n_2+1,n_2+1}$, and a scalar ρ such that the following optimization problem has a solution:

$$\min \rho \quad \text{s.t.}$$

$$\begin{bmatrix} \langle P\tilde{A} - U\tilde{C}\rangle + I_{n_2+1} & -(U\tilde{D} + P\tilde{I}) \\ \star & -\rho Q \end{bmatrix} \prec 0, \tag{6}$$

$$\rho > 0, \quad P \succ 0$$

where $U = [U_1^\top,\ U_2^\top]^\top$, then the selection of gains in (3) as $\tilde{L} = P^{-1}U$ renders the estimation error (4) asymptotically stable.

Proof: This proof follows the same ideas as in Beale and Shafai (1989), and thus is merely sketched. Consider (4) *and let* $V = e^\top Pe$ *be a candidate Lyapunov function. Computing the time derivative of* V*, one gets*

$$\dot{V} = \begin{bmatrix} e \\ d \end{bmatrix}^\top \underbrace{\begin{bmatrix} \langle P\tilde{A} + \tilde{L}\tilde{C}\rangle & -(\tilde{L}\tilde{D} + P\tilde{I}) \\ \star & 0 \end{bmatrix}}_{\Pi} \begin{bmatrix} e \\ d \end{bmatrix}. \tag{7}$$

indicating that the stability condition to be verified is $\Pi \prec 0$*. Now, to impose an optimizing criterion regarding the transfer* $d \mapsto e$*, the following criterion can be considered:*

$$\dot{V} + e^\top e - \gamma^2 d^\top Q d < 0$$

where γ *is a positive constant. The inequality* (6) *is then readily obtained by recalling* (7)*, and introducing the variables* $U = P\tilde{L}$ *and* $\rho = \gamma^2$*.* □

The choice of Q allows the designer to weigh the influence of each disturbance component. Indeed, higher gains L_1 and L_2 would reduce the impact of $\dot{w}$ on the estimation error, but deteriorate its sensitivity to measurement noise.

Remark 2. Let us highlight the nuances of the proposed approach. For simplicity, let $w = 0$ and assume that, for a given T_1, an observer gain $L = T_1L_r$ exists and renders both $A - LC$ and $A_r - L_rC_{m,r}$ stable. If the overall estimation error, *i.e.*, $\varepsilon = x - T_1\hat{x}_r$, is analyzed, one would get the following error dynamics:

$$T_1^\top \dot{\varepsilon} = T_1^\top (A - LC)\varepsilon - T_1^\top Lv$$

where clearly the projector T_1 "hides" some components, making any optimization pointless. Also, the fact that such equation has, at least, one dimension directly proportional to n, renders the search for L numerically cumbersome.

For these reasons, and as highlighted by the scheme in Fig. 1, the observer design is based solely on the reduced-order model. While solving the issue of the dimension, it raises a problem of interpretation: the reduced-state x_r has no physical meaning. Although its estimate $\hat{x}_r$ could be scaled-up on the large subspace, *i.e.*, $\hat{x} = T_1\hat{x}_r$, a part of the information on the large state cannot be recovered. This information loss is why the estimate of the reduced state is merely an intermediary step to recover the virtual output y_l, whose physical meaning (*i.e.*, the bending moments) is preserved during reduction.

3.3 $\mathcal{H}_\infty$ dynamic controller

In this section, we discuss the design of the robust controller responsible for alleviating the effect of the gust w over the loads y_l. Since *(i)* the estimation error dynamics (4) is independent of the control input, and *(ii)* the projector T_1 is obtained *beforehand*, the *separation principle* holds and thus the synthesis of the pair observer/controller can be carried out separately.

Also, this separation allows us to consider the (respective) virtual outputs $\tilde{y}_l$ as available for design. The real values fed to this controller, however, will be estimated by the observer in the implementation of the architecture.

The controller $K \in \mathcal{K}$ envisaged can be found as the solution of the following optimization problem:

$$K = \arg \min_{\bar{K} \in \mathcal{K} \subseteq \mathcal{H}_2} ||\mathcal{F}_l(G, \bar{K})||_{\mathcal{H}_\infty} \tag{8}$$

where G is a generalized plant that encompasses input/output weighting functions, $\mathcal{K} \subseteq \mathcal{H}_2$ is a subset meant to restrict the search of a controller to a given specific structure (here, a *stable dynamic controller*). Problem (8) can be solved through the `hinfstruct` routine in Matlab.

Let $T_{lw}(K)$ be the transfer function, accounting for the controller K, between the input w and the performance output $y_l^{(1)}$. Then, the generalized plant G above takes the following channels as constraints:

C1- The attenuation of the wind to load transfer peaks:
$$G_1 = W_l T_{lw}(K)$$
C2- Preservation of low-frequency characteristics (to avoid flight dynamics modification):
$$G_2 = W_e(T_{lw}(K) - T_{lw}(0))$$
where $T_{lw}(0)$ denotes the (stable) open-loop transfer.
C3- Stability and roll-off of the controller:
$$G_3 = W_k K$$

The first constraint relates to the objective on robustness, while the second ensures that handling qualities (or *maneuverability*) of the aircraft remain unaffected and, finally, the third ensures the stability of the controller.

4. NUMERICAL EXPERIMENT

In this section, we evoke the CRM/FERMAT configuration, as described in Quero et al. (2019), to illustrate the proposed methodology. In particular, we choose the mass case corresponding to 100 % of fuel mass with a mass equal to the maximum take-off weight of 260 tons. Regarding the structural part, a total of two symmetric (due to the imposed vertical gust encounter) rigid-body modes corresponding to the heave and pitch motions and 16 symmetric flexible modes are contained in a frequency interval which ranges from 1.0774 (Hz) up to 16.3742 (Hz) have been considered.

As for the aerodynamic model, the Doublet-Lattice Method (DLM), which models the unsteady compressible inviscid flow, has been employed. A total of 1910 aerodynamic panels represent lifting surfaces, and the effect of deflecting inboard and outboard ailerons and elevators is considered by properly modifying the corresponding downwash. The transfer of forces and displacements is done through a spline matrix based on the Thin Plate Splines (TPS). For more details regarding the configuration the reader is referred to Quero et al. (2019).

In this section we will design the observer (3) and evaluate its effectiveness and, then, implement it along the controller obtained from (8). The performance will then be analyzed against several scenarios of wind perturbations modelled as the *"1-cosine"* profile (see Fig. 2 below), *i.e.*,

$$w = \begin{cases} \dfrac{W_g}{2}\left(1 - \cos\left(\dfrac{V_a \pi}{L} t\right)\right), & \text{for } 0 \le t \le \dfrac{2L}{V_a} \\ 0, & \text{for } t > \dfrac{2L}{V_a} \end{cases} \tag{9}$$

where W_g is the gust velocity, L is the gust wavelength (ranging from 30 to 350 feet), and V_a is the aircraft true airspeed. The Mach number is 0.86, the flight altitude 9100 meters, and $W_g = 2$ m/s. Furthermore, all the upcoming simulation results will consider the measurement noise given by $v = 0.01\sin(100t) + \text{randn}(0, 10^{-2})$.

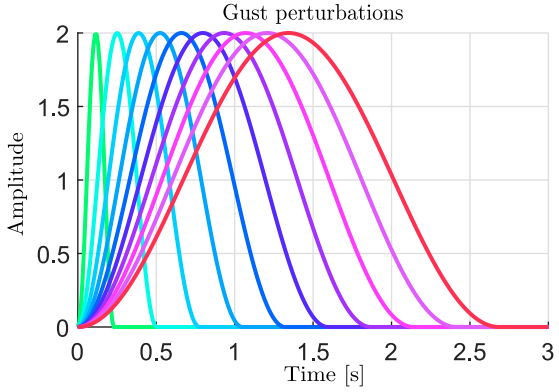

Fig. 2. Illustration of the gust perturbation considered.

4.1 Evaluation of the observer

The virtual outputs to be estimated are $\hat{y}_l = \text{vec}(y_l^1, y_l^{10}, y_l^{20})$. This selection stands as a design choice, whereas a dedicated method to this attention is a subject of future research.

Following Section 3.1, we select several orders n_2 ranging from 40 to 70, and compute the respective projectors T_1 and T_2 using BT. Then, the reduced-order system (2) and the *virtual* measurement matrix $C_l T_1$ (needed in (5)) are obtained. Furthermore, by selecting $Q = diag(10^1, 10^8)$, we use YALMIP (Löfberg, 2004) and the solver SDPT3 (Toh et al., 1999) to solve (6) and obtain observer (3).

By simulating the system in an open-loop setting, Fig. 3 illustrates the worst-case relative error for the estimation. As readily seen, the error becomes significantly low (below 7%) for an order $n_2 \geq 55$, for all the three desired estimates.

4.2 Evaluation of the control algorithm

The control synthesis is carried out following Section 3.3. The main objective is to attenuate the bending moment acting on the wing root (*i.e.*, $y_l^{(1)}$), which is wing station the most solicited by these loads. Therefore, for synthesis

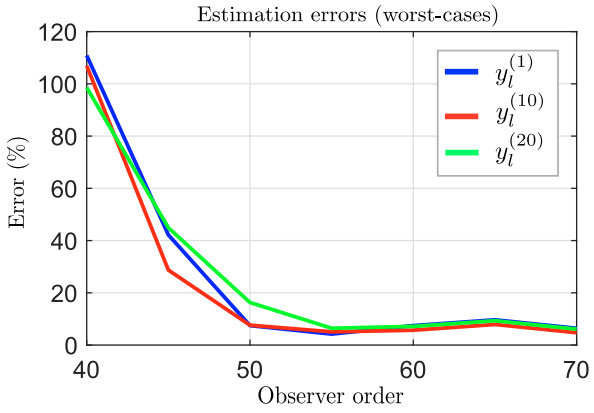

Fig. 3. Worst-case relative estimation error.

purposes, it is assumed that the transfer T_{lw} encompasses solely this specific channel.

To establish a comparison and highlight the advantage of having these estimates, two control configurations are implemented:

- *Controller 1*: proposed in this paper, and uses the estimated bending moments as virtual fed-back measurements;
- *Controller 2*: proposed by Poussot-Vassal et al. (2021), which has similar objectives but uses solely y_m as available feedback information.

Following Section 3.3, the synthesis of both controllers will be carried out using the following performance filters:

$$W_l = \|T_{lw}(0)\|_\infty^{-1}, \qquad W_e = G_e^{-1}\left(\frac{\frac{G_e}{\omega_0}s+1}{\frac{1}{\omega_0}s+1}\right)^2$$

$$W_k = 0.25\frac{s/\omega_a+1}{s/(10\omega_a)+1}$$

where $\omega_a = 2\pi f_a$, with $G_e = 0.1$ and $\omega_0 = 1$rad/s. We select the roll-off frequency $f_a = 5$Hz.

To compare both configurations, let an improvement index be given as

$$\text{Improv} = \frac{||T_{lw}(0)||_\infty - ||T_{lw}(K)||_\infty}{||T_{lw}(0)||_\infty}.$$

The obtained improvement indexes were 54.8% for *Controller 1*, and 28.3% for *Controller 2*. This is seen in Fig. 4, which compares the singular values of the original open-loop (*i.e.*, $T_{lw}(0)$), and the obtained closed-loop (*i.e.*, $T_{lw}(K)$) using both control configurations. As it can be seen, the worst-case peak is attenuated for both cases, but *Controller 1* shows enhanced performance. On the other hand, *Controller 1* have a bigger impact on the lower frequencies (below 0.1 rad/s) than *Controller 2*.

In the following, we compute the (worst-case) load envelope through time simulations. These simulations consider several realizations of gust, as described by (9). Furthermore, we fix the order of the observer as $n_2 = 60$.

Fig. 5 compares the obtained performance in contrast to the open-loop case. Controller 1, in general, offers a considerable attenuation of the bending moments throughout the wing. Controller 2, however, suffers from the influence

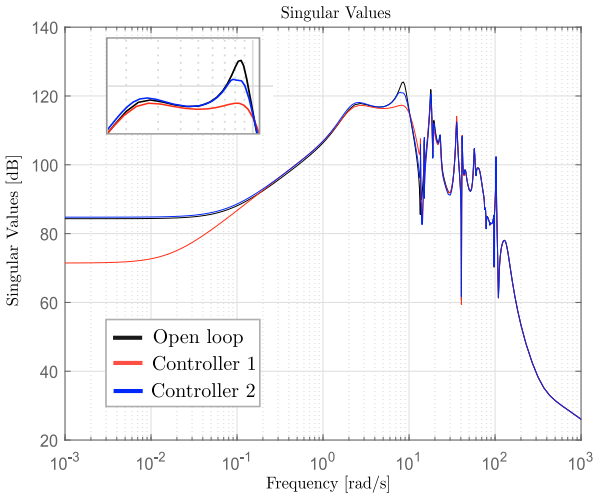

Fig. 4. Comparison of the singular values of T_{lw} on the original open-loop, and each controller configuration. The zoomed box highlights the peak of the transfer.

of measurement noise, which leads to poorer performance in several of the considered scenarios. This is explained by the fact that, by feed-backing the (estimated) virtual outputs $\hat{y}_l$, the gains of the controller regarding the actual measurements y_m (plagued by noise) are much smaller. Noise enters *Controller 1* mostly through the PIO (3), which acts also as a filter.

Finally, Fig. 6 illustrates the real and the estimated bending moments acting on the wing root, for a gust computed with a wavelength of $L = 350$ ft. The zoomed boxes highlight that all estimates degrade slightly when the effect of the unknown input is more substantial, whereas only the first estimate is sensitive to the measurement noise.

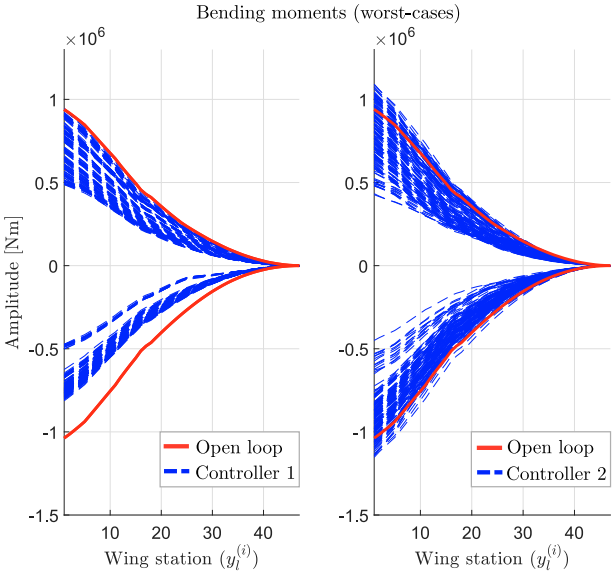

Fig. 5. Comparison of the performance obtained by each controller configuration, in terms of downward and upward bending moments.

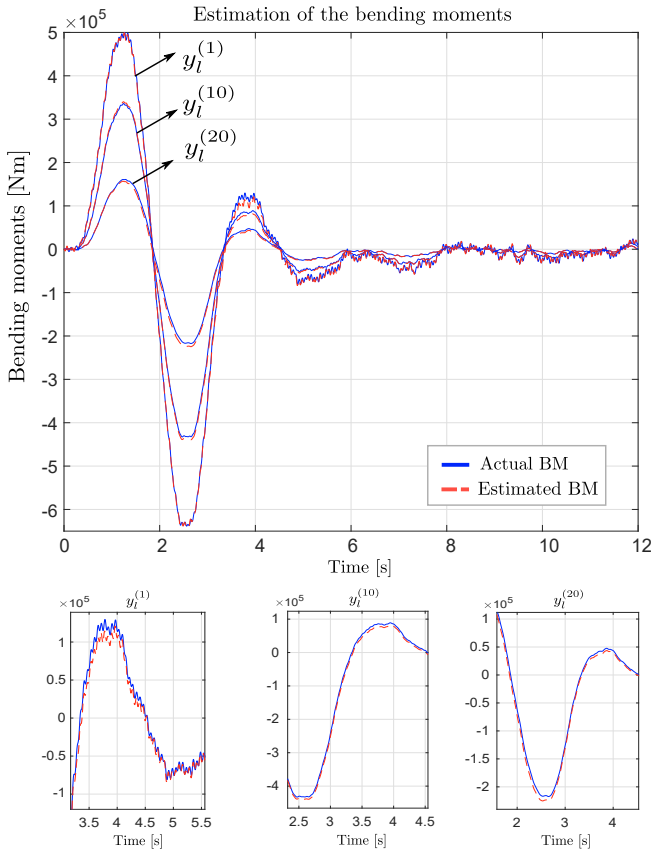

Fig. 6. Comparison between the real bending moments (BM) and its estimates. The boxes below highlights the worst error segments.

5. CONCLUSION

In this paper, we have investigated a methodology for the design of an active control aiming at the alleviation of gust loads in an aircraft. The proposed scheme encompasses a robust PI observer and a structured $\mathcal{H}_\infty$ controller. Since the original aeroelastic model is complex and high-dimensional, we perform the design of both observer and controller using a reduced-order model. The proposed framework allows us to estimate the bending moments acting on the wing and use them in a feedback fashion with the robust controller.

The methodology presented in this paper raises interesting questions. Future work foresees further investigation on the observer design and the optimization of its gains, as well as an extension to the parametric case, *i.e.*, considering a model describing several flight conditions. Also, a formalization of the stability of the high-dimensional system, as well as a procedure to select the best bending moments to be estimated and used in the control design is envisaged.

REFERENCES

Antoulas, A.C. (2005). *Approximation of Large-Scale Dynamical Systems*. Advances in Design and Control. SIAM.

Apkarian, P. and Noll, D. (2006). Nonsmooth H_∞ synthesis. *IEEE Transactions on Automatic Control*, 51(1), 71–86. doi:10.1109/TAC.2005.860290.

Beale, S. and Shafai, B. (1989). Robust control system design with a proportional integral observer. *International Journal of control*, 50(1), 97–111.

Cook, R.G., Palacios, R., and Goulart, P. (2013). Robust gust alleviation and stabilization of very flexible aircraft. *AIAA journal*, 51(2), 330–340.

Giesseler, H.G., Kopf, M., Varutti, P., Faulwasser, T., and Findeisen, R. (2012). Model predictive control for gust load alleviation. *IFAC Proceedings Volumes*, 45(17), 27–32.

Hansen, J.H., Duan, M., Kolmanovsky, I., and Cesnik, C.E. (2020). Control allocation for maneuver and gust load alleviation of flexible aircraft. In *AIAA Scitech 2020 Forum*, 1186.

Karpel, M. (1982). Design for active flutter suppression and gust alleviation using state-space aeroelastic modeling. *Journal of Aircraft*, 19(3), 221–227.

Livne, E. (2018). Aircraft active flutter suppression: State of the art and technology maturation needs. *Journal of Aircraft*, 55(1), 410–452.

Löfberg, J. (2004). Yalmip : A toolbox for modeling and optimization in matlab. In *In Proceedings of the CACSD Conference*. Taipei, Taiwan.

Poussot-Vassal, C., Vuillemin, P., Cantinaud, O., and Seve, F. (2021). Interpolatory methods for generic bizjet gust load alleviation function. *SIAM J. Appl. Dyn. Syst.*, 20(4), 2391–2411.

Quero, D., Vuillemin, P., and Poussot-Vassal, C. (2019). A generalized state-space aeroservoelastic model based on tangential interpolation. *Aerospace*, 6(1). doi:10.3390/aerospace6010009. URL `https://www.mdpi.com/2226-4310/6/1/9`.

Regan, C.D. and Jutte, C.V. (2012). Survey of applications of active control technology for gust alleviation and new challenges for lighter-weight aircraft. Technical report, NASA.

Sadamoto, T., Ishizaki, T., and Imura, J.i. (2013). Low-dimensional functional observer design for linear systems via observer reduction approach. In *52nd IEEE Conference on Decision and Control*, 776–781. doi:10.1109/CDC.2013.6759976.

Sadamoto, T., Ishizaki, T., and Imura, J.i. (2014). Projective state observers for large-scale linear systems. In *2014 European Control Conference (ECC)*, 2969–2974. doi:10.1109/ECC.2014.6862383.

Steiner, T. and Liu, S. (2020). Observer design for interconnected systems with model reduction and unknown inputs. *IFAC-PapersOnLine*, 53(2), 4169–4174. doi:https://doi.org/10.1016/j.ifacol.2020.12.2459. 21st IFAC World Congress.

Toh, K.C., Todd, M.J., and Tütüncü, R.H. (1999). Sdpt3 — a matlab software package for semidefinite programming, version 1.3. *Optimization Methods and Software*, 11(1-4), 545–581. doi:10.1080/10556789908805762.

Wang, Y., Song, H., Pant, K., Brenner, M.J., and Suh, P.M. (2016). Model order reduction of aeroservoelastic model of flexible aircraft. In *57th AIAA/ASCE/AHS/ASC Structures, Structural Dynamics, and Materials Conference*, 1222.

Zeng, J., Moulin, B., De Callafon, R., and Brenner, M.J. (2010). Adaptive feedforward control for gust load alleviation. *Journal of Guidance, control, and dynamics*, 33(3), 862–872.